

# Decomposition of austenite into pearlite from $\alpha+\gamma$ phase in steels having different microstructures before intercritical annealing

Hiroshi Hasegawa<sup>1</sup>, Hiroshi Matsuda<sup>2</sup>, Takako Yamashita<sup>1</sup> and Shinjiro Kaneko<sup>1</sup>

<sup>1</sup>JFE Steel Corporation, Steel Research Laboratory, 1, Kawasaki-cho, Chuo-ku, Chiba, 260-0835, Japan

<sup>2</sup>JFE Steel Corporation, Steel Research Laboratory, 1, Minamiwatarida-cho, Kawasaki-ku, Kanagawa, 210-0855, Japan

Dual-phase steel sheets composed of martensite and ferrite are widely applied in automotive body parts because of their high strength and superior ductility. It is important to suppress the pearlite formation from austenite ( $\gamma$ ) prior to martensite transformation by proper alloy design and heat-treatment pattern control in order to obtain target properties stably. This study aims to reveal the characteristics of the pearlite transformation behavior from  $\gamma$  having  $\alpha-\gamma$  grain boundaries. 0.14%C-1.5%Si-3.1%Mn (mass%) steel was used. Some characteristic  $\alpha-\gamma$  grain boundaries were intentionally formed by intercritical annealing at 973K from as-rolled microstructure of upper bainite and martensite (Steel R) and quenched-tempered microstructure of martensite and lower bainite (Steel L).  $\gamma$  grains were formed on polygonal ferrite grain boundaries in Steel R, but on prior  $\gamma$  grain boundaries (PAGBs) and packet/block/lath boundaries in Steel L during intercritical annealing. Pearlite transformation occurred randomly from polygonal ferrite /  $\gamma$  interface into  $\gamma$  in Steel R at 823K. On the other hand, it occurred mainly from  $\gamma$  formed on PAGBs, but hardly occurred from the  $\gamma$  formed on packet/block/lath boundaries in Steel L at 823K. No significant differences were observed concerning the concentration of alloying elements in  $\gamma$  grains formed between on the PAGBs and on the packet/block/lath boundaries in Steel L. The  $\gamma$  grains between polygonal ferrite grains or on PAGBs would not necessarily have orientation relationships such as Kurdjumov-Sachs relationship with all adjacent ferrite grains. On the other hand, the  $\gamma$  grains formed on the packet/block/lath boundaries would have orientation relationships with all adjacent ferrite grains by generating  $\gamma$  with the same crystal orientation as a prior austenite due to austenite memory phenomenon. These results may indicate pearlite formation is affected by the orientation relationships between the  $\gamma$  and surrounded phases.

**Keywords:** pearlite transformation, dual-phase steel, intercritical annealing, Kurdjumov-Sachs relationship

## 1. Introduction

Dual-phase (DP) steel sheets composed of martensite and ferrite are widely applied in automotive body parts because of their high strength and superior ductility. It is important to suppress the pearlite formation from austenite ( $\gamma$ ) prior to martensite transformation by proper alloy design and heat-treatment pattern control in order to obtain target properties stably. Many studies have been reported concerning pearlite transformation from  $\gamma$  single phase<sup>1,2)</sup>, in which the transformation starts from  $\gamma-\gamma$  grain boundary. This study aims to reveal the characteristics of the pearlite transformation behavior from  $\gamma$  with  $\alpha-\gamma$  grain boundaries.

## 2. Experiment

0.14%C-1.5%Si-3.1%Mn (mass%) steels were used in this study. Slabs were reheated at 1523K for 3.6ks and hot-rolled to 4mm in sheet thickness at a finish rolling temperature of 1163K. The hot-rolled sheets were cooled to 773K by water and kept for 3.6ks, subsequently cooled to room temperature in a furnace to obtain the microstructure consist of upper bainite and martensite. Both side of hot-rolled sheets were ground to a thickness of 3.2mm. These sheets were cold-rolled to a thickness of 1.0mm followed by annealing in a salt bath. Some specimens were annealed at 973K for 3.6ks from as-rolled microstructure of upper bainite and martensite and quenched into a salt bath kept at 823K for 0~1.8ks followed by water quenching. The other specimens were heat-treated at 1173K for 0.18ks and cooled to room temperature by air cooling to obtain the microstructure consist of martensite and lower bainite, subsequently annealed at 973K for 3.6ks and quenched into a salt bath kept at 823K for 0~1.8ks followed by water

quenching. Some characteristic  $\alpha-\gamma$  grain boundaries were intentionally formed by intercritical annealing at 973K from as-rolled microstructure of upper bainite and martensite (Steel R) and quenched-tempered microstructure of martensite and lower bainite (Steel L). Volume fraction of  $\gamma$  during annealing at 973K was about 34%. Carbon content in  $\gamma$  was about 0.4mass% in equilibrium state calculated by a Thermo-calc for this steel. Since this  $\gamma$  is exceeds Ac<sub>m</sub> line at 823K,  $\gamma$  is expected to transform into pearlite without ferrite transformation. After the heat treatment, the microstructures were observed by an optical microscope and a scanning electron microscope (SEM) after polishing and nital-etching. The crystal orientations were measured by an electron back-scatter diffraction (EBSD). The distributions of elements in microstructures were measured by a field emission gun electron microprobe analyzer (FE-EPMA).

## 3. Results

### 3.1 Microstructures before holding at 823K

The microstructure of the specimen water-quenched after annealing at 973K for 3.6ks is shown in Figure 1. In Steel R, the microstructure was composed of polygonal ferrite, cementite ( $\theta$ ) and martensite. Martensite grains, which were austenite at the annealing temperature, were mainly situated on the ferrite grain boundaries or the triple junctions of ferrite grains. The volume fraction of martensite was about 23%. The difference between observed fraction of martensite and calculated fraction of austenite by Thermo-calc would be attributed to  $\theta$  remaining in ferrite matrix. The mean widths of martensite grains were about 1-5 $\mu$ m. On the other hand, in Steel L, the microstructure was composed of ferrite and elongated martensite. Martensite particles were considered to be

mainly situated on the prior  $\gamma$  grain boundaries (PAGBs) or the packet, block, lath boundaries<sup>3)</sup> of martensite and lower bainite before annealing. The volume fraction of martensite was about 31% closing to the calculated value by Thermo-calc. Mean widths of martensite gains were under 1 $\mu$ m. Finer martensite grains were obtained in Steel L than that in Steel R.

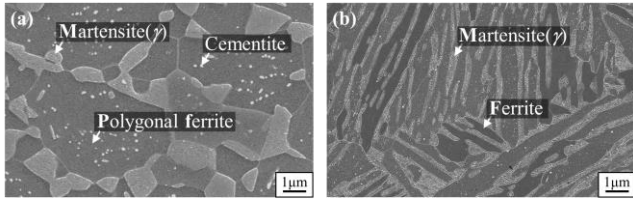


Figure 1 Microstructures of (a) Steel R and (b) Steel L after annealing at 973K for 3.6ks followed by water quenching.

### 3.2 Microstructure change during holding at 823K

Microstructures held at 823K followed by water quenching were shown in figure 2. In Steel R, a slight amount of pearlite was observed in the 0.06ks-held specimen, larger pearlite grains were observed in the specimen held for 0.18ks or more. In Steel L, pearlite was not observed in the 0.06ks-held and 0.18ks-held specimen, a small amount of pearlite was observed in the 0.6ks-held specimen. Pearlite transformation occurred randomly from polygonal ferrite /  $\gamma$  interface into  $\gamma$  in Steel R. On the other hand, it occurred intensively in the limited area on the specific boundaries in Steel L. In addition, the amount of ferrite was at a constant and bainite was not observed in any specimens.

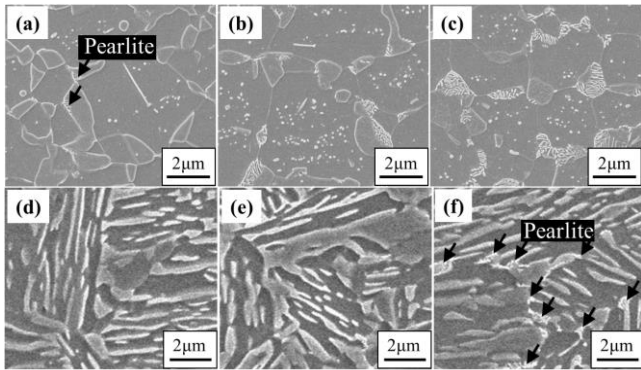


Figure 2 Microstructures after holding at 823K for (a) 0.06ks, (b) 0.18ks, (c) 0.6ks in Steel R and for (d) 0.06ks, (e) 0.18ks, (f) 0.6ks in Steel L followed by water quenching.

## 4. Discussion

### 4.1 Characteristics of pearlite transformation site

Pearlite transformation occurred randomly from polygonal ferrite /  $\gamma$  interface into  $\gamma$  in Steel R at 823K. On the other hand, it occurred intensively in the limited area on the specific boundaries in Steel L. The features of this specific boundaries were analyzed from a crystallographic point of view. Figure 3 shows crystal orientations of regions A and B sandwiching the region where pearlite intensively formed and pole figures of regions A and B. Pole figures of regions A and B indicate that the orientation of prior  $\gamma$  is different each other. Therefore, it was found that the specific boundaries where pearlite intensively formed were PAGBs.

This results also indicate that pearlite transformation is less likely occur from  $\gamma$  formed on packet, block, lath boundaries than that on PAGBs.

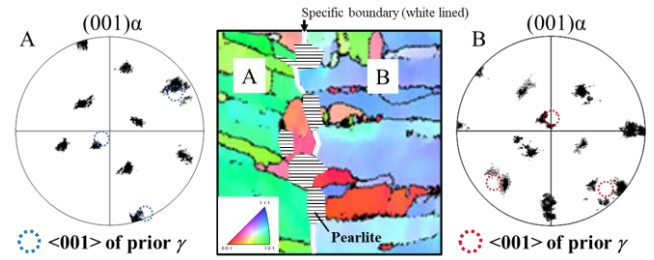


Figure 3 Crystal orientations of region A, B sandwiching the region where pearlite formed intensively and the pole figures of region A, B in Steel L. Pearlite regions and specific boundary are illustrated on the crystal orientation map.

### 4.2 Affecting factors of pearlite formation

The effect of carbon and manganese content in  $\gamma$  on the decomposition of  $\gamma$  were investigated. Figure 4 shows SEM images and carbon, manganese maps before holding at 823K. Carbon and manganese were enriched in martensite and correspond to the same region in both Steel R and Steel L. Carbon and manganese content in  $\gamma$  was higher in Steel R than that in Steel L. Since manganese suppress the pearlite transformation<sup>2)</sup>, manganese content in  $\gamma$  was not a dominant factor on faster start of pearlite transformation in Steel R than Steel L. In hypo-eutectoid steel, it has been reported that the pearlite transformation from the  $\gamma$  single phase starts with the formation of ferrite<sup>1)</sup>. However, in the case of pearlite transformation from  $\alpha + \gamma$  binary phase, formation of  $\theta$  may be a dominant factor of onset of the pearlite transformation because of no need for ferrite nucleation. Such mechanism enables to explain the faster start of pearlite transformation in Steel R due to high carbon content in  $\gamma$  in this research. On the other hand, since there was no significant difference in the amount of carbon and manganese between the  $\gamma$  on the PAGBs and on the other site, intensive formation of pearlite in  $\gamma$  on PAGBs is due to the other factors.

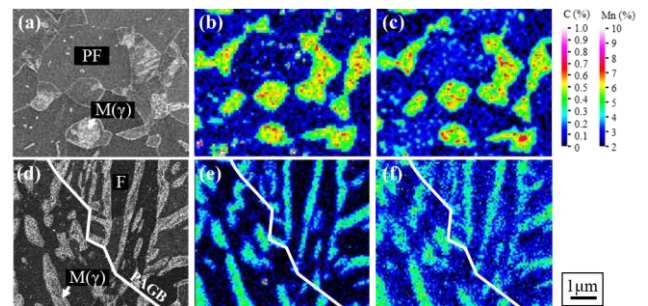


Figure 4 Microstructures and alloying element maps before holding at 823K; (a) SEM image, (b) carbon map, (c) manganese map of Steel R and (d) SEM image, (e) carbon map, (f) manganese map of Steel L. PAGBs are illustrated on images as white lines.

Orientation relationships between  $\alpha$  and  $\gamma$  may affect on the nucleation of pearlite through interfacial energy<sup>4)</sup>. While the  $\gamma$  grains between polygonal ferrite grains or on PAGBs would not necessarily have orientation relationships such as Kurdjumov-Sachs relationship<sup>5)</sup> with all adjacent ferrite grains, the  $\gamma$  grains formed on the packet,

block, lath boundaries would have orientation relationships with all adjacent ferrite grains by generating  $\gamma$  with the same crystal orientation as a prior austenite due to austenite memory phenomenon.

## 5. Summary

Pearlite transformation behavior from ferrite and austenite binary phase by intercritical annealing from an as-rolled microstructure (Steel R) and a quenched-tempered microstructure (Steel L) was investigated. Pearlite transformation was suppressed in Steel L compared to Steel R. In addition, pearlite formation was further suppressed in  $\gamma$  not on prior  $\gamma$  grain boundaries in Steel L. Suppression of pearlite transformation in Steel L than in Steel R would be caused by carbon content in  $\gamma$ . Further suppression of pearlite transformation in Steel L was not explained by the effect alloying elements and these concentration. Orientation relationships between  $\alpha$  and  $\gamma$  may affect on the nucleation of pearlite through interfacial energy.

Control the microstructure before intercritical annealing into a low temperature microstructure such as martensite or bainite without deformation is one of the effective methods.

## 6. References

- 1) M. Hillert: *Decomposition of Austenite by Diffusional Processes*, Interscience, (1962), 197-237.
- 2) E. C. Bain: *Alloying elements in Steel*, (1954).
- 3) I. Tamura, Y. Nariyoshi, S. Shimooka and Y. Nakajima: *Tetsu-to-Hagané*, **64** (1978), 568-577.
- 4) W. C. Johnson, C. L. White, P. E. Marth, P. K. Ruf, S. M. Tuominen, K. D. Wade, K. C. Russell and H. I. Aaronson: *Metall. Trans. A*, **6A** (1975), 911.
- 5) G. Kurdjumov, G. Sachs: *Z. Phys.* **64**(1930), 325-343.